

Rnf functions in generation of a proton gradient in *Desulfovibrio alaskensis*

Luyao Wang, Peter Bradstock, Chuang Li, Michael J McInerney, Lee R Krumholz

Rnf is a membrane protein complex that oxidizes reduced ferredoxin and reduces NAD^+ with the energy released during this exergonic reaction used to generate a proton motive force. Here, *Desulfovibrio alaskensis* G20 and Rnf mutants of G20 were grown with different electron donor and acceptor combinations to determine the importance of Rnf in energy conservation and the type of ion gradient generated. Addition of the protonophore TCS strongly inhibited lactate-sulfate dependent growth whereas the sodium ionophore ETH2120 had no effect, suggesting the importance of a proton gradient in energy conservation. Mutants in *rnfA* and *rnfD* were more sensitive to the protonophore at 5 μM than the parental strain, suggesting the importance of Rnf in the generation of a proton gradient. The electrical potential ($\Delta\Psi$), ΔpH and proton motive force were lower in the *rnfA* mutant than in the parental strain of *D. alaskensis* G20. These results provide evidence that the Rnf complex in *D. alaskensis* functions as a primary proton pump whose activity is important for growth.

Rnf functions in Generation of a Proton Gradient in *Desulfovibrio alaskensis*

*Luyao Wang¹, Peter Bradstock¹, Chuang Li¹, Michael J. McInerney¹, Lee R.
Krumholz^{1,2*},*

Department of Botany and Microbiology¹ and Institute for Energy and the
Environment²,

The University of Oklahoma, Norman, OK 73019 and

Running title:

*Corresponding author:

Department of Microbiology and Plant Biology, The University of Oklahoma,
770 Van Vleet Oval, Norman, OK 73019, USA

Tel: 405-325-0437 Fax: 405-325-7619 Email: krumholz@ou.edu

Contents category: Microbial metabolism

ABSTRACT

Rnf is a membrane protein complex that oxidizes reduced ferredoxin and reduces NAD^+ with the energy released during this exergonic reaction used to generate a proton motive force. Here, *Desulfovibrio alaskensis* G20 and Rnf mutants of G20 were grown with different electron donor and acceptor combinations to determine the importance of Rnf in energy conservation and the type of ion gradient generated. Addition of the protonophore TCS strongly inhibited lactate-sulfate dependent growth whereas the sodium ionophore ETH2120 had no effect, suggesting the importance of a proton gradient in energy conservation. Mutants in *rnfA* and *rnfD* were more sensitive to the protonophore at 5 μM than the parental strain, suggesting the importance of Rnf in the generation of a proton gradient. The electrical potential ($\Delta\Psi$), ΔpH and proton motive force were lower in the *rnfA* mutant than in the parental strain of *D.alaskensis* G20. These results provide evidence that the Rnf complex in *D. alaskensis* functions as a primary proton pump whose activity is important for growth.

45 The Rnf complex was first discovered in *Rhodobacter capsulatus* and is thought to be
 46 transcribed in one cluster of seven genes *rnfABCDGEH* (Jouanneau et al. 1998).
 47 Evidence that depleting one subunit could destabilize others indicated the formation of a
 48 complex (Kumagai et al. 1997) which was later shown to be a membrane-bound
 49 complex involved in the *Rhodobacter* nitrogen fixation process (Schmehl et al. 1993).
 50 The Rnf complex has been differentiated into three major groups based on gene
 51 organization (Biegel et al. 2011). The first group found in *R. capsulatus*, *Pseudomonas*
 52 *stutzeri* (Yan et al. 2008) and *Azotobacter vinelandii* (Curatti et al. 2005) with
 53 *rnfABCDGE*. Another group with the gene order *rnfCDGEAB* is found in *A. woodii*
 54 (Biegel et al. 2009) and *Clostridium kluyveri* (Seedorf et al. 2008). Lastly *rnfBCDGEA*
 55 is found in *Chlorobium limicola*, *Bacteroides vulgatus* and *Prosthecochloris aestuarii*
 56 (Biegel et al. 2011).

57 Rnf complex has been shown to be a novel type of ferredoxin-dependent enzyme,
 58 catalyzing the oxidation-reduction reaction between reduced ferredoxin and NAD^+
 59 (Biegel et al. 2009; Boiangiu et al. 2005). Because of the high sequence similarity to the
 60 Na^+ -translocating NADH:ubiquinone oxidoreductase (Nqr) (Kumagai et al. 1997), the
 61 Rnf complex in *R. capsulatus* was suggested to be involved in ion translocation using
 62 the energy from the exergonic reduction of NAD^+ coupled to the oxidation of reduced
 63 ferredoxin (Müller et al. 2008). Based on the above similarity, Rnf was originally
 64 proposed to be a sodium pump (Biegel et al. 2009). This theory was strengthened after
 65 the Rnf complex in *Acetobacterium woodii* was confirmed to generate a Na^+ gradient
 66 when carrying out the redox reaction between reduced ferredoxin and NAD^+ (Biegel &
 67 Müller 2010). However, the Rnf complex was suggested to be a proton-translocating

68 ferredoxin:NAD⁺ oxidoreductase in *Clostridium ljungdahlii* (Kopke et al. 2010) and
69 was more recently shown to produce a proton gradient (Tremblay et al. 2013). It
70 therefore appears that Rnf may pump different ions in different bacteria (Buckel &
71 Thauer 2013).

72 *Desulfovibrio alaskensis* G20 encodes the Rnf complex with a unique gene
73 arrangement (*rnf*CDGEABF); however, a similar Rnf complex is present in most
74 sulfate-reducing bacteria for which genome sequences are available (Pereira et al. 2011).
75 The first gene in the *rnf* operon is a decaheme cytochrome (DhcA) that belongs to
76 cytochrome c₃ family (Pereira et al. 2011). The final gene in the operon, *rnfF* is most
77 similar to *apbE*, a membrane associated lipoprotein (Beck & Downs 1999).

78 Recently, it was reported that mutants in Rnf in *D. alaskensis* are unable to grow
79 using H₂ or during syntrophic growth conditions with *Syntrophus aciditrophicus* or
80 *Syntrophomonas wolfeii* (Krumholz et al. 2015b; Price et al. 2014). By investigating
81 gene expression levels of *D. alaskensis* G20 grown in pure culture or under syntrophic
82 conditions (Krumholz et al. 2015b), it was suggested that both formate and H₂ can act
83 as electron shuttles during syntrophic growth. Those experiments also showed that
84 expression of *rnf* genes are upregulated under syntrophic conditions and during H₂
85 dependent growth confirming the role of the Rnf complex in H₂ metabolism.

86 In this experiment, mutants of RnfA (Dde_0585) and RnfD (Dde_0582) were
87 studied and compared with the G20 parent strain to determine whether Rnf in *D.*
88 *alaskensis* is involved in generation of a proton motive force (PMF). These two
89 mutants of *Desulfovibro alaskensis* G20 were obtained by using mini Tn10 transposon

(Groh et al. 2005) and identified individually during syntrophic growth with *Syntrophomonas wolfeii* (Krumholz et al. 2015b).

MATERIALS AND METHODS

Growth of Cultures. *Desulfovibrio alaskensis* G20 and *rnf* mutants were routinely cultured anaerobically (N₂-CO₂, 80:20) in basal medium with lactate-sulfate (50mM each) as the electron donor and electron acceptor, respectively and contained 0.1% yeast extract (Krumholz et al. 2015b). The medium was prepared under a headspace of N₂/CO₂ (80/20, vol/vol) with sodium bicarbonate (3.5g/L) added as a buffer. Before inoculation, the medium was reduced with 0.025% each cysteine and sulfide. Kanamycin (1050 µg/mL) was added to the mutant cultures. Inoculum consisted of 0.2 ml transferred into 10 ml of media or the same ratio for large volume cultures. Cultures were grown in the incubator at 37°C and growth of triplicate cultures was measured by optical density at 600 nm. The stock cultures were frozen in 20% glycerol at -20°C. Growth of syntrophic cocultures was as previously described (Krumholz et al. 2015b).

Growth was tested with a variety of other electron donors and acceptors: lactate (50mM), pyruvate (25mM), ethanol (10mM) and formate (50mM). Sulfate was used at 50mM with lactate and 25mM with other electron donors and sulfite was added at 10mM.

The protonophore 3,3,4,5-tetrachlorosalicylanide (TCS, 5 µM or 20 µM), or the sodium-specific ionophore N,N,N',N'-Tetracyclohexyl-1,2-phenylenedioxydiacetamide (ETH2120, 20 µM) were added to media to test their effects on growth.

113 **Transcriptional analysis of *rnf* genes.** Total RNA was extracted from the parent strain,
 114 *rnfA*, and *rnfD* mutants using the Qiagen RNeasy kit as previously described (Krumholz
 115 et al. 2015b). Purity and adequate yield was confirmed with a diode-array
 116 spectrophotometer. First-strand cDNA synthesis was performed using the Fermentas
 117 Revertaid kit with gene-specific primers covering the entirety of the *rnf* mutants'
 118 operons. Primers were designed to span the gaps between each gene in the operon
 119 (Table 1). PCR was performed with the parent strain and mutants with each primer set
 120 followed by agarose gel analysis to determine whether all genes in the operon were
 121 expressed and whether the genes were on the same transcript.

122 *Quantitative PCR analysis.* Triplicate cultures of the parent strain and *rnfA* and *rnfD*
 123 mutants were grown to mid-log phase (OD₆₀₀ 0.3-0.45) and harvested by centrifugation
 124 at 5,000 x g for 5 min at 4 C. The pellet was homogenized in RNAprotect Bacteria
 125 reagent (QIAGEN) for 5 min at room temperature to prevent degradation of RNA
 126 transcripts. Excess liquid was removed by centrifugation and cell pellets were
 127 resuspended in 200ul of TE buffer containing 1mg/ml lysozyme. Total RNA was
 128 extracted using the RNeasy mini kit (QIAGEN). RNA was then treated with the
 129 Ambion Turbo DNA –free kit (Thermo) to eliminate genomic DNA contamination.
 130 RNA was quantified spectrophotometrically. cDNAs were synthesized using the First
 131 Stand cDNA synthesis kit (Fermentas) as described in the manual. Control PCR
 132 reactions were done to ensure there was no genomic DNA or non-specific
 133 amplification.

134 Quantitative PCR, was done in triplicate from each culture replicate using 10ng
 135 cDNA as the template and the Maxima SYBR Green qPCR master mix (Thermo) with a

136 MyIQ Cycler (Bio-Rad). Primers were designed using Primer-BLAST (NCBI website)
 137 to specifically amplify 128- to 155-bp regions of targeted genes Dde_587, Dde_589,
 138 Dde_590 (Table 2). Dde_587 is the final gene in the *rnf* operon and the other two
 139 genes are the next two ORFs directly downstream of the operon. The 16s rRNA
 140 primers were as previously described (Li et al. 2011). Reactions used the following
 141 amplification condition: 95C for 10 min; 40 cycles of denaturation at 95C for 15 s and
 142 annealing/extension at 60C for 1 min. mRNA expression was calculated using $(E_{\text{target}})^{\Delta$
 143 $\text{ar_target (control- treated)} / (E_{\text{reference}})^{\Delta \text{Ct_reference (control- treated)}}$ (Pfaffl 2001) The 16s rRNA gene
 144 was used for normalization.

145 **Washed cell experiments.** Washed cells were used to measure sulfide production
 146 under non-growth conditions. Briefly, 100 ml lactate-sulfate culture grown to mid
 147 log phase was harvested by centrifugation at 5300 x g for 15 min, washed twice in
 148 buffer containing 50 mM MOPS (pH 7.2), 5 mM MgCl₂ and resuspended in the same
 149 buffer. All buffers were flushed with N₂ for 30 min. Assays were carried out in
 150 serum tubes containing 2 ml of buffer-cell mixture incubated at 37°C on a shaker at
 151 100rpm. The assay mixture contained the washing buffer, 5mM sodium sulfate and
 152 either 50 mM lactate, 50 mM sodium formate (N₂ headspace) or H₂ in the headspace.
 153 Between 50 and 200 µg of cell protein was added to each tube. Tubes were sacrificed
 154 by addition of 2 ml 10% Zinc Acetate at 60 min intervals for sulfide analysis. Sulfide
 155 was determined using the methylene blue assay (Cline 1969).

156 **Measurement of proton motive force.** Triplicate cultures of *D. alaskensis* parent strain
 157 and *rnfA* mutant were grown in lactate –sulfate basal medium until mid logarithmic
 158 phase (OD₆₀₀ of 0.5) in a 1 liter volume and 30 ml aliquots of cells were dispensed into

159 100ml serum bottles under N₂/CO₂ (80/20, vol/vol). Protein concentration was
160 determined using the Bicinchoninic Acid Assay (Pierce BCA Protein Assay Kit).

161 Transmembrane electrical potential ($\Delta\Psi$) was measured as previously described
162 (Tremblay et al. 2013). Briefly, cells were incubated with
163 [³H]tetraphenylphosphonium bromide ([³H]TPP⁺) (ARC, 0.1 μ Ci/ml) for 15 min at 37°C
164 (Kashket & Barker 1977; Shirvan et al. 1989). [³H]TPP⁺ was dissolved in media and
165 filtered through 0.45 μ m filters prior to adding to cells. Controls were incubated with
166 nigericin (ACROS ORGANICS, 20 μ M dissolved in ethanol at 200x) and valinomycin
167 (ACROS), 20 μ M dissolved in DMSO at 200x) for 15 min to eliminate the $\Delta\Psi$. The
168 combination of nigericin (proton/K⁺ antiporter) and valinomycin (K⁺ uncoupler) will
169 dissipate the proton gradient (Kessler et al. 1977). Cells were then separated from
170 the medium using silicone oil as described below and [³H]TPP⁺ was determined in the
171 liquid scintillation counter (Packard TriCarb 2100TR). The uptake of [³H]TPP⁺ was
172 corrected for extracellular contamination using the ratio of the intracellular to
173 extracellular volume as described below. Non-specific binding of [³H]TPP⁺ was
174 corrected by subtracting the cell associated [³H]TPP⁺ in the valinomycin/nigericin
175 treatment from that in the untreated cells. The $\Delta\Psi$ was calculated with the simplified
176 Nernst equation ($-2.3 [RT/F] \times \log[(\text{concentration in})/(\text{concentration out})]$).

177 The Δ pH was measured by testing the distribution of [¹⁴C]benzoate (ARC,
178 0.4 μ Ci/ml) across the cell membrane after 15min incubation at 37°C with cells
179 (Kashket & Barker 1977; Shirvan et al. 1989). Cells were then separated from the
180 supernatant as described below and [¹⁴C]benzoate was measured. [¹⁴C]benzoate
181 uptake was corrected for extracellular contamination using the ratio of intracellular to

182 extracellular volume described below. Tetrachlorosalicylanilide (TCS, 20 μ M) was
 183 added to controls to eliminate the Δ pH and was used to calculate internal pH in the
 184 absence of a Δ pH. The external pH was measured, [14 C]benzoate uptake was
 185 quantified and intracellular pH was calculated with the Henderson–Hasselbach equation
 186 (Rottenberg 1979). The proton motive force (PMF) was calculated using the equation:
 187 $PMF = \Delta\Psi - z\Delta pH$. At 37°C, z equals to 61.48.

188 ***Measurement of intracellular volume/total volume of cell pellet.*** 3H_2O (1 μ Ci/ml)
 189 was used to measure the total pellet volume while [14 C]taurine (PerkinElmer, 0.5 μ Ci/ml)
 190 was used to measure extracellular volume and was inferred to penetrate up to the
 191 plasma membrane (Kashket & Barker 1977). The intracellular water volume was
 192 estimated from total pellet water volume minus extracellular water volume by
 193 measuring the difference between the distribution of 3H_2O and [3H]taurine after
 194 incubating cells for 15 min at 37°C with each isotope.

195 ***Separation of cells from the supernatant.*** Following the 15 minute incubation with
 196 the isotope, three 10 ml aliquots of the total 30 ml solution were put into three 15 ml
 197 Falcon tubes with 3ml of a mixture of silicone oils (25% Fluid 510, 50 centistokes, and
 198 75% Fluid 550, 115 centistokes; Dow-Corning Corp, Serva. vol/vol). Cells were then
 199 centrifuged at 5300 x g at 4°C for 10min. The aqueous layer and the silicone oil was
 200 removed with a Pasteur pipette connected to a vacuum line. The bottom of the falcon
 201 tube containing the cell pellet was cut off and moved into the scintillation vial and the
 202 cell pellet was re-suspended with 200 μ l distilled-water. Liquid scintillation cocktail
 203 (PerkinElmer, Ultima Gold) was added prior to scintillation counting.

204 **Statistical analysis.** Statistical analysis used either the t-test or a one-way analysis of
205 variance (ANOVA) with the Tukey's Range test.

206 RESULTS

207 **Mutants in the *rnf* operon.** In a previous study, a Tn10 mutant library of *D.*
208 *alaskensis* G20 was screened for the ability to grow on butyrate in coculture with
209 *Syntrophomonas wolfei* (Krumholz et al. 2015b). Seventeen mutants were obtained
210 that were deficient in syntrophic growth. Of these, two mutants had the transposon
211 insertions within a putative *rnf* operon. This operon is composed of 8 genes located on
212 the genome as shown in Table 3 and genes appear to be co-transcribed. They are
213 separated from the nearest upstream transcribed region by 185 bps and from the nearest
214 downstream transcribed region by 342 bps. The two syntrophy mutants had
215 transposon insertions within *rnfA* and *rnfD* as determined using Arbitrary PCR
216 (Krumholz et al. 2015b). Both genes encode integral membrane proteins likely located
217 in the cytoplasmic membrane. RnfD has been previously shown to bind a flavin
218 (Biegel et al. 2011).

219 **Transcriptional analysis of the *rnf* operon.** The complete transcriptional analysis for
220 strain G20 under lactate-sulfate, H₂-sulfate and under syntrophic growth conditions has
221 been previously published (Krumholz et al. 2015b). Here we present a summary of
222 normalized values for transcription of each subunit within the *rnf* operon (Table 3).
223 Transcription of all genes in the operon are similar under each condition and are
224 affected similarly by growth condition. The most highly expressed genes are the first
225 two in the operon, the gene for the cytochrome c family protein and *rnfC*, both of which
226 have 1.5-2 fold higher levels of expression than genes for the other subunits.

227 Expression was also enhanced approximately 2-fold when cultures were grown on H₂,
 228 relative to lactate, indicating the importance of this protein for H₂ dependent growth.
 229 Syntrophic cultures had enhanced expression of all eight genes compared to
 230 lactate/sulfate growth with similar levels of expression in the *S. aciditrophicus* coculture
 231 to H₂-grown cells and higher levels of expression observed in the *S. wolfei* coculture,
 232 indicating the importance of this protein complex under syntrophic conditions.

233 ***Expression analysis of rnf operons in mutants.*** To determine whether the
 234 transposon insertion eliminated downstream expression of genes in the *rnf* operon, gap
 235 analysis was performed where all intergene regions were amplified except the region
 236 between *rnfB* and *rnfA* using cDNA prepared using mRNA. All of the intergene
 237 regions were amplified for the parent and the two mutants (Fig. S1) confirming that the
 238 genes form an operon and indicating that the mutants likely have intact transcripts of the
 239 interrupted operon. In this operon, the insertions are likely only affecting the one
 240 interrupted gene.

241 We carried out RT-PCR analysis of the terminal gene in the operon, Dde_587
 242 (*apbE*) as well as the two genes that followed that operon, Dde_589 (*uspA*) and
 243 Dde_590 (*cls*) to be certain that downstream expression was not affected by the
 244 insertions. Expression of the terminal gene in the operon was impacted in the
 245 mutants with a 4 fold decrease in expression in the *rnfA* mutant and a 2 fold
 246 increase in the *rnfD* mutant (Table 4). The following 2 genes were minimally
 247 impacted indicating that the insertions present in the mutants likely do not affect
 248 downstream expression.

249 ***Growth and sulfate reduction by rnf mutants.*** The two mutants exhibited similar
 250 growth rates to that of the parent strain when lactate was the electron donor with sulfate
 251 (Fig. 1A) or sulfite as electron acceptor (Fig. 1B). When pyruvate was the donor,
 252 growth yields were reduced for the mutants (Fig. 1C). We previously reported that *rnf*
 253 mutants grew poorly (*rnfD*) or not at all (*rnfA*) on H₂ (Krumholz et al. 2015b; Fig. S2)
 254 and a recent study has reported that *rnf* mutants grow poorly or not at all with sulfate as
 255 the electron acceptor on malate, fumarate, ethanol, hydrogen, and formate, but growth is
 256 not affected in lactate and pyruvate (Price et al. 2014). Here, it is shown that the *rnfD*
 257 mutant has a long lag phase with formate as the donor, but eventually grew to a similar
 258 OD to the parent strain (Fig. 1D). The *rnfA* mutant did not grow on formate or H₂
 259 clearly indicating the involvement of Rnf in formate/H₂-dependent growth. We also
 260 confirmed that the *rnfA* mutant will not grow on ethanol (Fig. S3).

261 ***Sulfide production by washed cells.*** Washed cells were used to determine if the role for
 262 *rnf* was linked to biosynthesis, as mutants were able to grow better on more complex
 263 carbon compounds. Incubations of washed cells of the parent strain and the *rnfA*
 264 mutant produced 0.57 and 0.17 $\mu\text{mol sulfide}\cdot\text{hr}^{-1}\cdot\text{mg}^{-1}$ protein respectively with lactate
 265 as electron donor. Addition of either 5 μM TCS to the washed cells of the parent
 266 strain prevented 95% of the sulfide production and addition of 20 μM to washed cells
 267 inhibited sulfide production by 100%, suggesting TCS directly disrupts the proton
 268 gradient needed for respiration. With H₂ as the electron donor, parent strain cells
 269 produced 0.30 $\mu\text{mol sulfide}\cdot\text{hr}^{-1}\cdot\text{mg}^{-1}$ protein whereas the *rnfA* mutant did not have any
 270 detectable activity. To further test whether the lack of growth on H₂ was due to the
 271 mutant's inability to biosynthesize carbon intermediates, we attempted to grow the

272 mutant and the parent strain with H₂ as the electron donor with 0.1% Casamino acids
 273 added to the media. The mutant would still not grow (Fig. S4), providing further
 274 evidence that the role for RNF was not directly linked to biosynthesis.

275 ***Growth curves with ionophores.*** The sodium ion ionophore ETH 2120, tested at 20
 276 μ M, did not have a significant influence on the growth of the parent strain or the *rnf*
 277 mutants with lactate as the electron donor whether sulfate or sulfite were present as
 278 electron acceptors (Fig S5,S6). Interestingly, the protonophore, TCS , at 5 μ M
 279 differentially inhibited cultures (Fig. 2). TCS partially inhibited the growth of the parent
 280 strain and completely inhibited the growth of *rnf* mutants on lactate-sulfate (Fig. 2A and
 281 Fig. S5). Growth on lactate sulfite was then tested and 5 μ M TCS was shown to have
 282 a smaller but still significant inhibitory effect on growth in the parent strain (Fig. 2B)
 283 and again completely inhibited the *rnfA* mutant (Fig. 2B, S6). A higher level of TCS
 284 was then tested and it was shown that 20 μ M TCS almost completely inhibited the
 285 growth of the parent strain on lactate-sulfite (Fig. 2B) and again completely inhibited
 286 the mutants (Fig. S7).

287 ***Measurement of $\Delta\Psi$, ΔpH and PMF.*** To determine whether the Rnf complex is
 288 involved in the formation of a proton gradient, the transmembrane potential ($\Delta\Psi$), ΔpH
 289 and proton motive force (PMF) were measured in cells of the G20 parent strain and the
 290 *rnfA* mutant growing on lactate-sulfate. The $\Delta\Psi$ and ΔpH were both reduced in the
 291 mutant (Table 5), which led to a significantly lower PMF in the *rnfA* mutant relative to
 292 the G20 parent strain. The lower ΔpH and PMF in the *rnfA* mutant shows that the Rnf
 293 complex clearly had an impact on the energy conservation system by affecting the
 294 proton gradient.

DISCUSSION

The Rnf complex has previously been shown to catalyze the oxidation-reduction reaction between ferredoxin and NAD^+ (Biegel et al. 2009; Boiangiu et al. 2005). Reduced ferredoxin has a redox potential ($E'=-400\text{mV}$) (Lovenberg et al. 1963; Smith et al. 1991; Yoch & Valentine 1972) that is more negative than that of NAD^+/NADH couple ($E'=-280\text{mV}$) and therefore the transfer of electrons by Rnf from reduced ferredoxin to NAD^+ releases sufficient energy to generate either a proton or a sodium ion potential (Buckel & Thauer 2013). Given that recent studies have demonstrated both proton (Tremblay et al. 2013) and Na^+ translocation abilities (Biegel & Müller 2010), it was imperative to determine which ion Rnf translocates in strain G20. Growth experiments showed that lactate-sulfate grown cells were insensitive to the Na^+ ionophore, ETH2120, (Figs. S5, S6) but were highly sensitive to the protonophore, TCS (Fig. 2). Resting cells were also shown to be highly sensitive to TCS suggesting that the proton gradient is needed for respiration. A similar growth profile was observed in *C. ljungdahlii*, for which this result was interpreted to infer that a proton gradient was needed for growth (Tremblay et al. 2012).

When grown on lactate-sulfate or lactate-sulfite, TCS partially inhibited the growth of the parent strain and completely inhibited the growth of *rnfA* and *rnfD* mutants (Fig. 2). The stronger effect on the mutants suggested that TCS at $5\text{ }\mu\text{M}$ was partially dissolving the proton gradient in the parent strain and this was confirmed when cells were shown to be completely inhibited at $20\mu\text{M}$ TCS. We would therefore expect that at $5\text{ }\mu\text{M}$ TCS, growth processes requiring additional proton motive force (or ATP synthesis) would be more highly inhibited than those requiring less ATP. The use of

sulfate as an electron acceptor initially requires energy to activate sulfate to adenosine-5'-phosphosulfate (Gavel et al. 1998). The requirement for energy to activate sulfate may explain why lactate-sulfate grown cells are more susceptible to the action of TCS than are lactate-sulfite-grown cells as the proton gradient generated during sulfate respiration would be needed to make ATP for sulfate activation. The inability of *rnf* mutants to grow in the presence of 5 uM TCS is consistent with its role in the generation of a proton motive force. In fact, the magnitude of the proton motive force in *rnf* mutants is much less than that in the parent strain of G20 (Table 5).

Ideally, we would have generated complemented *rnf* mutants to prove that the observed insertions were not having polar effects on other genes. We have attempted to clone the *rnfA* and *rnfD* genes into *Escherichia coli* as the first step in complementing the mutants. Unfortunately we have not been successful. Another group has experienced similar problems with *rnfAB* of *Clostridium ljungdahlii* and suggested that *rnf* genes may be toxic to *E. coli* in some cases (Tremblay et al. 2013). Gap analysis was used to show that the insertions did not block transcription of downstream genes providing some evidence that polar effects are not important. As well, we carried out RT-PCR analysis of downstream genes and showed, that the insertions have little effect on expression.

Experiments reported here and elsewhere (Price et al. 2014) show that the *rnf* mutants are unable to grow on H₂, formate and ethanol. These results point to a critical role for Rnf in generation of a proton gradient during growth on the above substrates and are consistent with a higher expression level of *rnf* genes when growing with H₂ and sulfate relative to lactate and sulfate (Table 3).

341 A proton gradient is thought to be generated during H₂ metabolism in *Desulfovibrio*
 342 (Badziong & Thauer 1980) and used for the synthesis of ATP. Membrane vesicle
 343 experiments carried out in our lab in an attempt to demonstrate the generation of an ion
 344 gradient coupled to the oxidation of reduced ferredoxin and reduction of NAD⁺ have
 345 been unsuccessful. The protein product of the decaheme cytochrome that precedes the
 346 *rnf* operon has been proposed to accept electrons from hydrogenases and shuttle them to
 347 Rnf (Matias et al. 2005; Pereira et al. 2011). However, mutants in this gene had no
 348 effect on fitness during growth experiments on ethanol, formate or H₂ (Price et al. 2014).
 349 This suggests that Rnf is not likely receiving electrons directly from H₂. It is more
 350 likely that *D. alaskensis* relies extensively on ferredoxin oxidation by Rnf to produce a
 351 proton gradient during growth on substrates that do not yield net ATP by substrate-level
 352 phosphorylation. For those substrates that do yield ATP by substrate level
 353 phosphorylation such as malate, fumarate, pyruvate and lactate, a decreased growth rate
 354 and or yield was observed in most cases for *rnf* mutants (Fig. 1)(Price et al. 2014)
 355 suggesting that both Rnf and the F₁F_o ATPase are involved in generating a PMF under
 356 those conditions.

357 We are not familiar with any studies describing mechanisms of ferredoxin
 358 reduction in *Desulfovibrio*, however, several possible mechanisms have been suggested
 359 (Pereira et al. 2011; Price et al. 2014). During H₂ oxidation, these include a possible
 360 cytoplasmic electron-bifurcating hydrogenases-linked to a heterodisulfide reductase for
 361 which mutants grow poorly on H₂ and formate (Hdr/flox-1). For ethanol oxidation,
 362 the acetaldehyde:ferredoxin oxidoreductase could be used, and with pyruvate and
 363 lactate oxidation, would involve pyruvate:ferredoxin oxidoreductase.

364 This study has shown that the *D. alaskensis* Rnf complex mostly likely functions as
365 a proton rather than a sodium pump and is essential for growth on substrates that do not
366 involve ATP synthesis by substrate-level phosphorylation. Mutation of Rnf limits the
367 development of the PMF and, thus, affects ATP synthesis during growth.

368

369

REFERENCES

- 370 Badziong W, and Thauer RK. 1980. Vectorial electron transport in *Desulfovibrio*
371 *vulgaris* (Marburg) growing on hydrogen plus sulfate as sole energy source.
372 *Archives of Microbiology* 125:167-174.
- 373 Beck BJ, and Downs DM. 1999. A periplasmic location is essential for the role of the
374 ApbE lipoprotein in thiamine synthesis in *Salmonella typhimurium*. *Journal of*
375 *Bacteriology* 181.
- 376 Biegel E, and Müller V. 2010. Bacterial Na⁺-translocating ferredoxin: NAD⁺
377 oxidoreductase. *Proceedings of the National Academy of Sciences*
378 107:18138-18142.
- 379 Biegel E, Schmidt S, González JM, and Müller V. 2011. Biochemistry, evolution and
380 physiological function of the Rnf complex, a novel ion-motive electron transport
381 complex in prokaryotes. *Cellular and Molecular Life Sciences* 68:613-634.
- 382 Biegel E, Schmidt S, and Müller V. 2009. Genetic, immunological and biochemical
383 evidence for a Rnf complex in the acetogen *Acetobacterium woodii*.
384 *Environmental Microbiology* 11:1438-1443.
- 385 Boiangiu CD, Jayamani E, Brügel D, Herrmann G, Kim J, Forzi L, Hedderich R,
386 Vgenopoulou I, Pierik A, and Steuber J. 2005. Sodium ion pumps and hydrogen
387 production in glutamate fermenting anaerobic bacteria. *Journal Molecular*
388 *Microbiology and Biotechnology* 10:105-119.
- 389 Buckel W, and Thauer RK. 2013. Energy conservation via electron bifurcating
390 ferredoxin reduction and proton/Na⁺ translocating ferredoxin oxidation.
391 *Biochimica et Biophysica Acta (BBA)-Bioenergetics* 1827:94-113.
- 392 Cline JD. 1969. Spectrophotometric Determination of Hydrogen Sulfide in Natural
393 Waters. *Limnology and Oceanography* 14:454-&.
- 394 Curatti L, Brown CS, Ludden PW, and Rubio LM. 2005. Genes required for rapid
395 expression of nitrogenase activity in *Azotobacter vinelandii*. *Proceedings of the*
396 *National Academy of Sciences* 102:6291-6296.
- 397 Gavel OY, Bursakov SA, Calvete JJ, George GN, Moura JIG, and Moura I. 1998. ATP
398 sulfurylases from sulfate-reducing bacteria of the genus *Desulfovibrio*. A novel
399 metalloprotein containing cobalt and zinc. *Biochemistry* 37:16225-16232.
- 400 Groh JL, Luo Q, Ballard JD, and Krumholz LR. 2005. A method adapting microarray
401 technology for signature-tagged mutagenesis of *Desulfovibrio desulfuricans*

402 G20 and *Shewanella oneidensis* MR-1 in anaerobic sediment survival
 403 experiments. *Applied and environmental microbiology* 71:7064-7074.

404 Jouanneau Y, Jeong HS, Hugo N, Meyer C, and Willison JC. 1998. Overexpression in
 405 *Escherichia coli* of the *rnf* genes from *Rhodobacter capsulatus*--characterization
 406 of two membrane-bound iron-sulfur proteins. *European Journal of Biochemistry*
 407 251:54-64.

408 Kashket E, and Barker SL. 1977. Effects of potassium ions on the electrical and pH
 409 gradients across the membrane of *Streptococcus lactis* cells. *Journal of*
 410 *Bacteriology* 130:1017-1023.

411 Kessler RJ, Vande Zande H, Tyson CA, Blondin GA, Fairfield J, Glasser P, and Green
 412 DE. 1977. Uncouplers and the molecular mechanism of uncoupling in
 413 mitochondria. *Proc Natl Acad Sci U S A* 74:2241-2245.

414 Kopke M, Held C, Hujer S, Liesegang H, Wiezer A, Wollherr A, Ehrenreich A, Liebl
 415 W, Gottschalk G, and Durre P. 2010. *Clostridium ljungdahlii* represents a
 416 microbial production platform based on syngas. *Proc Natl Acad Sci U S A*
 417 107:13087-13092.

418 Krumholz LR, Bradstock P, Sheik CS, Diao Y, Gazioglu O, Gorby Y, and McInerney
 419 MJ. 2015a. Syntrophic growth of *Desulfovibrio alaskensis* requires genes for H₂
 420 and formate metabolism as well as those for flagellum and biofilm
 421 formation. *Applied and environmental microbiology* 81:2339-2348.

422 Krumholz LR, Bradstock P, Sheik CS, Diao Y, Gazioglu O, Gorby Y, and McInerney
 423 MJ. 2015b. Syntrophic growth of *Desulfovibrio alaskensis* requires genes for H₂
 424 and formate metabolism as well as those for flagellum and biofilm formation.
 425 *Appl Environ Microbiol* 81:2339-2348.

426 Kumagai H, Fujiwara T, Matsubara H, and Saeki K. 1997. Membrane localization,
 427 topology, and mutual stabilization of the *rnfABC* gene products in *Rhodobacter*
 428 *capsulatus* and implications for a new family of energy-coupling NADH
 429 oxidoreductases. *Biochemistry* 36:5509-5521.

430 Li X, McInerney MJ, Stahl DA, and Krumholz LR. 2011. Metabolism of H₂ by
 431 *Desulfovibrio alaskensis* G20 during syntrophic growth on lactate. *Microbiology*
 432 157:2912-2921.

433 Lovenberg W, Buchanan BB, and Rabinowitz JC. 1963. Studies on the chemical nature
 434 of clostridial ferredoxin. *Journal of Biological Chemistry* 238:3899-3913.

435 Matias PM, Pereira IA, Soares CM, and Carrondo MA. 2005. Sulphate respiration from
 436 hydrogen in *Desulfovibrio* bacteria: a structural biology overview. *Progress in*
 437 *biophysics and molecular biology* 89:292-329.

438 Müller V, Imkamp F, Biegel E, Schmidt S, and Dilling S. 2008. Discovery of a
 439 ferredoxin:NAD⁺-oxidoreductase (Rnf) in *Acetobacterium woodii*: a novel
 440 potential coupling site in acetogens. *Annals of the New York Academy of*
 441 *Sciences* 1125:137-146.

442 Pereira IAC, Ramos AR, Grein F, Marques MC, Da Silva SM, and Venceslau SS. 2011.
 443 A comparative genomic analysis of energy metabolism in sulfate reducing
 444 bacteria and archaea. *Frontiers in Microbiology* 2:1-22.

445 Pfaffl MW. 2001. A new mathematical model for relative quantification in real-time
 446 RT-PCR. *Nucleic Acids Res* 29:e45.

- 447 Price MN, Ray J, Wetmore KM, Kuehl JV, Bauer S, Deutschbauer AM, and Arkin AP.
448 2014. The genetic basis of energy conservation in the sulfate-reducing bacterium
449 *Desulfovibrio alaskensis* G20. *Frontiers in Microbiology* 5.
- 450 Rottenberg H. 1979. [64] The measurement of membrane potential and ΔpH in cells,
451 organelles, and vesicles. *Methods in enzymology* 55:547-569.
- 452 Schmehl M, Jahn A, zu Vilsendorf AM, Hennecke S, Masepohl B, Schuppler M,
453 Marxer M, Oelze J, and Klipp W. 1993. Identification of a new class of nitrogen
454 fixation genes in *Rhodobacter capsulatus*: a putative membrane complex
455 involved in electron transport to nitrogenase. *Molecular and General Genetics*
456 *MGG* 241:602-615.
- 457 Seedorf H, Fricke WF, Veith B, Brüggemann H, Liesegang H, Strittmatter A, Miethke
458 M, Buckel W, Hinderberger J, and Li F. 2008. The genome of *Clostridium*
459 *kluverii*, a strict anaerobe with unique metabolic features. *Proceedings of the*
460 *National Academy of Sciences* 105:2128-2133.
- 461 Shirvan M, Schuldiner S, and Rottem S. 1989. Volume regulation in *Mycoplasma*
462 *gallisepticum*: evidence that Na^+ is extruded via a primary Na^+ pump. *Journal*
463 *of Bacteriology* 171:4417-4424.
- 464 Smith ET, Tomich JM, Iwamoto T, Richards JH, Mao Y, and Feinberg BA. 1991. A
465 totally synthetic histidine-2 ferredoxin: thermal stability and redox properties.
466 *Biochemistry* 30:11669-11676.
- 467 Tremblay P-L, Zhang T, Dar SA, Leang C, and Lovley DR. 2013. The Rnf complex of
468 *Clostridium ljungdahlii* is a proton-translocating ferredoxin: NAD^+
469 oxidoreductase essential for autotrophic growth. *Mbio* 4:e00406-00412.
- 470 Tremblay PL, Aklujkar M, Leang C, Nevin KP, and Lovley D. 2012. A genetic system
471 for *Geobacter metallireducens*: role of the flagellin and pilin in the reduction of
472 $Fe(III)$ oxide. *Environmental Microbiology Reports* 4:82-88.
- 473 Yan Y, Yang J, Dou Y, Chen M, Ping S, Peng J, Lu W, Zhang W, Yao Z, and Li H.
474 2008. Nitrogen fixation island and rhizosphere competence traits in the genome
475 of root-associated *Pseudomonas stutzeri* A1501. *Proceedings of the National*
476 *Academy of Sciences* 105:7564-7569.
- 477 Yoch DC, and Valentine RC. 1972. Four-iron (sulfide) ferredoxin from *Bacillus*
478 *polymyxa*. *Journal of Bacteriology* 110:1211-1213.

Table 1. List of primers used for gap analysis in the *rnf* operon.

Gap	Forward primer	Reverse primer
Gap CC (cytC/rnfC)	GGCATTCACGGCCTGTGCCT	CTTGTCGCCGGGGTGATCGG
Gap CD (rnfC/rnfD)	CCTGCTGGGACGCTACAGCG	ATGCCGTGTATGGTGCGCCC
Gap DG (rnfD/rnfG)	GGCAAGGCCGCCATGGTCAT	TGTACTCGGCCCCCGTGGAG
Gap GE (rnfG/rnfE)	ATCGGCTGCATGGTTGCCGT	ATTGGCGGACTTGGTGACCG
Gap EA (rnfE/rnfA)	GGGCTTGTCTGGGCGCCAT	CCGCCCATGCCCAGACTGAC
Gap BE (rnfB/ApbE)	AAAGCCTGCCTCGCGTTCGG	AAGCCCCAGCAGACCGCATG

494

Table 2. Primers used for the RT-qPCR experiments

Primer	Sequence	Target gene
Dde_587 forward	5'-AACCGTGGGTTATCGCCATT-3'	ApbE gene
Dde_587 reverse	5'-ATGGCTGTACATGCGTTTGC-3'	
Dde_589 forward	5'-AAGGGCAGGTAGTGCTGATG-3'	Putative regulator gene
Dde_589 reverse	5'-GGTAAACTTCACGCCTTCGC-3'	
Dde_590 forward	5'-GCCTGCGGCTTAATTTCGAG-3'	Cardiolipin synthase gene
Dde_590 reverse	5'-ACGGTTTTCCAGTTCGCTCA-3'	
16s forward	5'-ACGGTTGGAAACGACTGCTA-3'	16s rRNA gene
16s reverse	5'-AGCTAATCAGACGCGGACTC-3'	

496

Table 3. Normalized expression levels of genes within the *rnf* operon (from (Krumholz et al. 2015a)). Expression was determined with the parent strain of *D. alaskensis* G20 during growth in pure culture with the indicated electron donors and acceptors and in coculture with *S. aciditrophicus* (SB) or with *S. wolfei* (SW) in the presence of benzoate or butyrate, respectively, as electron donors and sulfate as the electron acceptor.

Gene	Function	Lactate/ Sulfate	H ₂ / Sulfate	H ₂ / Sulfite	SB	SW
Dde_0580	cyt c family protein	3.17	8.33	6.18	6.02	14.36
Dde_0581	RnfC subunit	3.05	6.68	6.12	5.61	13.50
Dde_0582	RnfD subunit	1.90	4.41	3.34	2.68	7.73
Dde_0583	RnfG subunit	2.83	6.35	5.19	5.43	10.07
Dde_0584	RnfE subunit	1.86	4.95	3.80	3.39	7.63
Dde_0585	RnfA subunit	2.24	5.78	4.23	2.98	8.41
Dde_0586	RnfB subunit	2.18	4.39	4.16	1.48	8.09
Dde_0587	ApbE	2.20	4.90	5.25	1.94	10.15

503

504

505

506

507

508

Table 4. Gene expression in *D. alaskensis rnfA* and *rnfD* mutants relative to the parental strain using RT-qPCR. And normalized with the 16s rRNA gene.

Mutant type	Dde_587	Dde_589	Dde_590
<i>rnfA</i>	0.227 ± 0.255	0.608 ± 0.097	0.589 ± 0.253
<i>rnfD</i>	1.955 ± 0.624	1.155 ± 0.078	0.972 ± 0.420

Table 5. Magnitude of the ΔpH , $\Delta \Psi$ and total proton motive force of the *D. alaskensis* G20 parent strain and the *rnfA* mutant growing on lactate and sulfate. Standard deviation in parentheses. Value for the *rnfA* mutant were statistically different from the parent strain at $p < 0.05$.

Measurement	Parent Strain	<i>rnfA</i> mutant
$\Delta \Psi$	-158 mV (2.1)	-117 mV (3.2)
ΔpH	0.43 (0.057)	0.29 (0.015)
PMF	-185 mV (3.1)	-135 mV (4.1)

Figures

Fig. 1

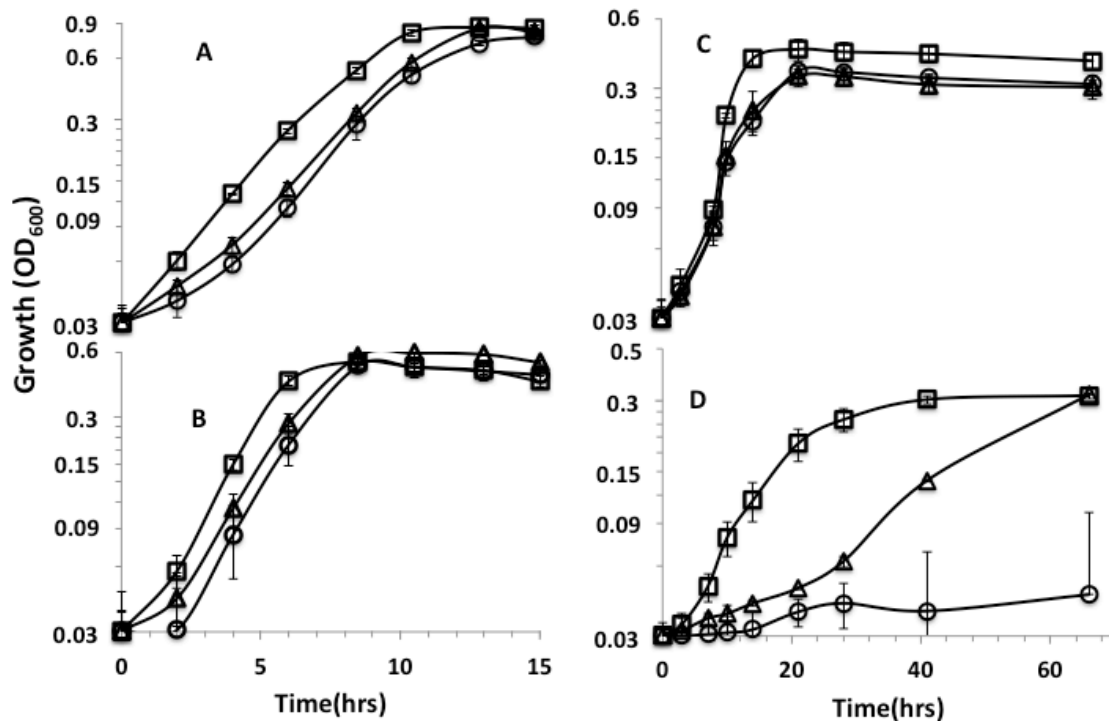


Figure 1. Growth curves on (A) lactate-sulfate (B) lactate-sulfite (C) pyruvate-sulfate and (D) formate-sulfate. Curves are for *D. alaskensis* parent strain (□) *rnfA* (○) and *rnfD* (△) mutants. Error bars show standard deviation.

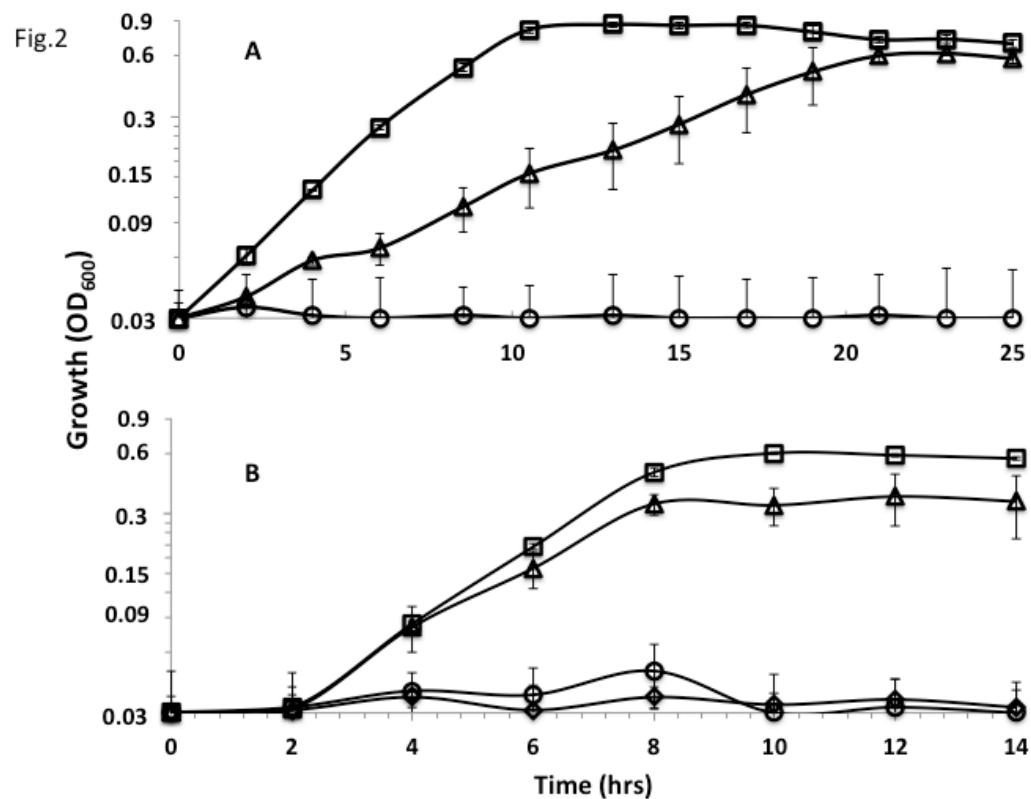


Figure 2. Growth curves with (A) lactate-sulfate and (B) lactate sulfite for *D. alaskensis* parent strain no addition (□) and with 5μM (△) or 20 μM (◇) TCS. Growth curve of the *rnfA* mutant with 5μM TCS (○) is also shown. Error bars show standard deviation.

Table 1 (on next page)

Table 1.

Table 1. List of primers used for gap analysis in the *rnf* operon.

1 Table 1. List of primers used for gap analysis in the *rnf* operon.

Gap	Forward primer	Reverse primer
Gap CC (cytC/rnfC)	GGCATTACGGCCTGTGCCT	CTTGTCGCCGGGGTGATCGG
Gap CD (rnfC/rnfD)	CCTGCTGGGACGCTACAGCG	ATGCCGTGTATGGTGCGCCC
Gap DG (rnfD/rnfG)	GGCAAGGCCGCCATGGTCAT	TGTACTCGGCCCCCGTGGAG
Gap GE (rnfG/rnfE)	ATCGGCTGCATGGTTGCCGT	ATTGGCGGACTTGGTGACCGC
Gap EA (rnfE/rnfA)	GGGCTTGTTCTGGGCGCCAT	CCGCCCATGCCCAGACTGAC
Gap BE (rnfB/ApbE)	AAAGCCTGCCTCGCGTTCGG	AAGCCCCAGCAGACCGCATG

2

Table 2(on next page)

Table 2.

Table 2. Primers used for the RT-qPCR experiments

1 Table 2. Primers used for the RT-qPCR experiments

Primer	Sequence	Target gene
Dde_587 forward	5'-AACCGTGGGTATCGCCATT-3'	ApbE gene
Dde_587 reverse	5'-ATGGCTGTACATGCGTTTGC-3'	
Dde_589 forward	5'-AAGGGCAGGTAGTGCTGATG-3'	Putative regulator gene
Dde_589 reverse	5'-GGTAACTTCACGCCTTCGC-3'	
Dde_590 forward	5'-GCCTGCGGCTTAATTTTCGAG-3'	Cardiolipin synthase gene
Dde_590 reverse	5'-ACGGTTTTCCAGTTCGCTCA-3'	
16s forward	5'-ACGGTTGGAAACGACTGCTA-3'	16s rRNA gene
16s reverse	5'-AGCTAATCAGACGCGGACTC-3'	

2
3

Table 3 (on next page)

Table 3.

Table 3. Normalized expression levels of genes within the *rnf* operon (from (Krumholz et al. 2015a)). Expression was determined with the parent strain of *D. alaskensis* G20 during growth in pure culture with the indicated electron donors and acceptors and in coculture with *S. aciditrophicus* (SB) or with *S. wolfei* (SW) in the presence of benzoate or butyrate, respectively, as electron donors and sulfate as the electron acceptor.

Table 3. Normalized expression levels of genes within the *rnf* operon (from (Krumholz et al. 2015a)). Expression was determined with the parent strain of *D. alaskensis* G20 during growth in pure culture with the indicated electron donors and acceptors and in coculture with *S. aciditrophicus* (SB) or with *S. wolfei* (SW) in the presence of benzoate or butyrate, respectively, as electron donors and sulfate as the electron acceptor.

Gene	Function	Lactate/ Sulfate	H ₂ / Sulfate	H ₂ / Sulfite	SB	SW
Dde_0580	cyt c family protein	3.17	8.33	6.18	6.02	14.36
Dde_0581	RnfC subunit	3.05	6.68	6.12	5.61	13.50
Dde_0582	RnfD subunit	1.90	4.41	3.34	2.68	7.73
Dde_0583	RnfG subunit	2.83	6.35	5.19	5.43	10.07
Dde_0584	RnfE subunit	1.86	4.95	3.80	3.39	7.63
Dde_0585	RnfA subunit	2.24	5.78	4.23	2.98	8.41
Dde_0586	RnfB subunit	2.18	4.39	4.16	1.48	8.09
Dde_0587	ApbE	2.20	4.90	5.25	1.94	10.15

Table 4(on next page)

Table 4.

Table 4. Gene expression in *D. alaskensis rnfA* and *rnfD* mutants relative to the parental strain using RT-qPCR. And normalized with the 16s rRNA gene.

Table 4. Gene expression in *D. alaskensis rnfA* and *rnfD* mutants relative to the parental strain using RT-qPCR. And normalized with the 16s rRNA gene.

Mutant type	Dde_587	Dde_589	Dde_590
<i>rnfA</i>	0.227 ± 0.255	0.608 ± 0.097	0.589 ± 0.253
<i>rnfD</i>	1.955 ± 0.624	1.155 ± 0.078	0.972 ± 0.420

Table 5 (on next page)

Table 5. Magnitude of the ΔpH , $\Delta\Psi$ and total proton motive force of the *D. alaskensis* G20 parent strain and the *rnfA* mutant growing on lactate and sulfate.

Table 5. Magnitude of the ΔpH , $\Delta\Psi$ and total proton motive force of the *D. alaskensis* G20 parent strain and the *rnfA* mutant growing on lactate and sulfate. Standard deviation in parentheses. Value for the *rnfA* mutant were statistically different from the parent strain at $p < 0.05$.

Table 5. Magnitude of the ΔpH , $\Delta\Psi$ and total proton motive force of the *D. alaskensis* G20 parent strain and the *rnfA* mutant growing on lactate and sulfate. Standard deviation in parentheses. Value for the *rnfA* mutant were statistically different from the parent strain at $p < 0.05$.

Measurement	Parent Strain	<i>rnfA</i> mutant
$\Delta\Psi$	-158 mV (2.1)	-117 mV (3.2)
ΔpH	0.43 (0.057)	0.29 (0.015)
PMF	-185 mV (3.1)	-135 mV (4.1)

Figure 1(on next page)

Figure 1-Growth curves of parent strain and mutants.

Figure 1. Growth curves on (A) lactate-sulfate (B) lactate-sulfite (C) pyruvate-sulfate and (D) formate-sulfate. Curves are for *D. alaskensis* parent strain (£) *rnfA* (□) and *rnfD* (r) mutants. Error bars show standard deviation.

Fig. 1

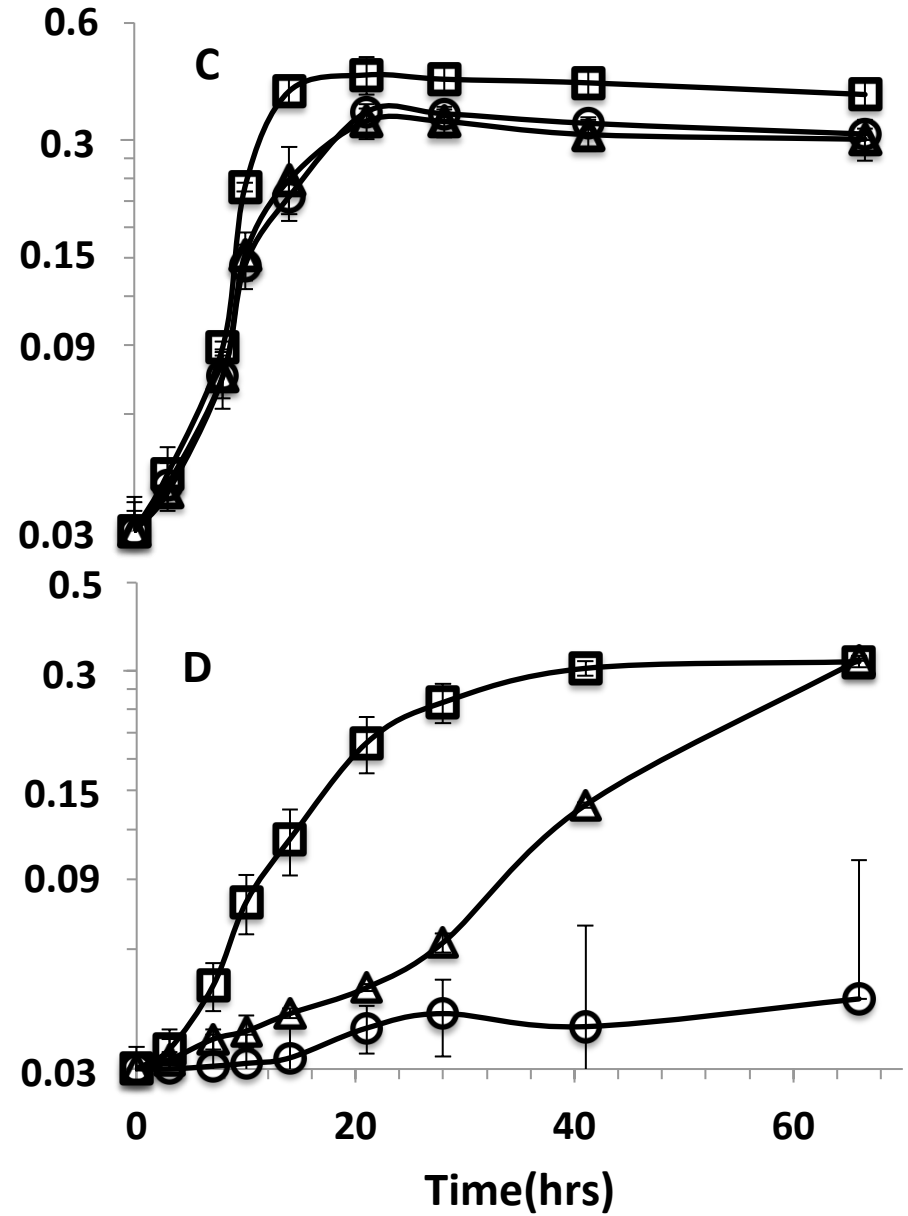
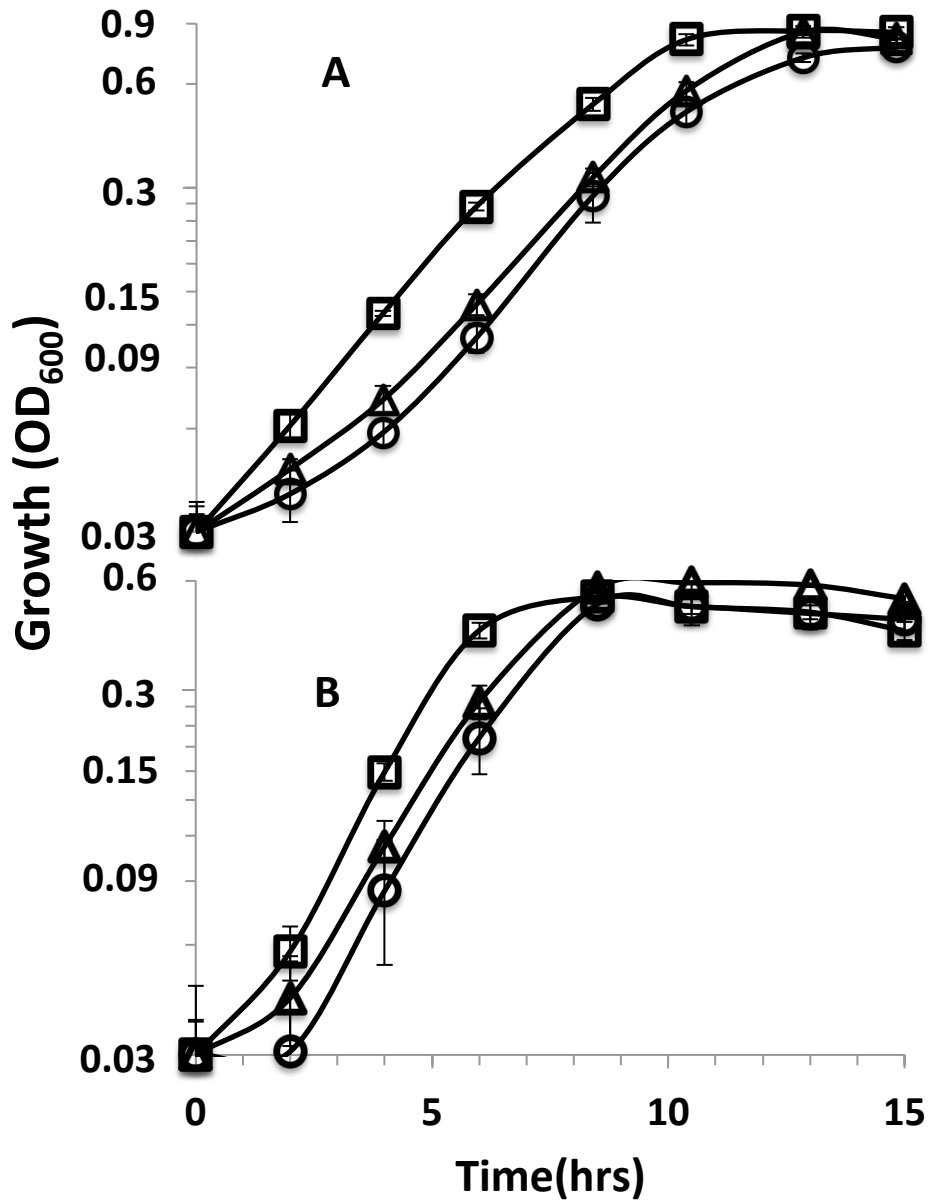


Figure 2 (on next page)

Figure 2. Effect of TCS on parent strain and mutants.

Figure 2. Growth curves with (A) lactate-sulfate and (B) lactate sulfite for *D. alaskensis* parent strain no addition (£) and with 5µM (r) or 20 µM (ˆ) TCS. Growth curve of the *rnfA* mutant with 5µM TCS (□) is also shown. Error bars show standard deviation.

Fig.2

